

AROW: A V2X-based Automated Right-of-Way Algorithm for Distributed Cooperative Intersection Management

Ghayoor Shah¹, Yaser P. Fallah¹, Danyang Tian², Ehsan Moradi-Pari²

Abstract—Safe and efficient intersection management is critical for an improved driving experience. As per several studies, an increasing number of crashes and fatalities occur every year at intersections. Most crashes are a consequence of a lack of situational awareness and ambiguity over intersection crossing priority. In this regard, research in Cooperative Intersection Management (CIM) is considered highly significant since it can utilize Vehicle-to-Everything (V2X) communication among Connected and Autonomous Vehicles (CAVs). CAVs can transceive basic and/or advanced safety information, thereby improving situational awareness at intersections. Although numerous studies have been performed on CIM, most of them are reliant on the presence of a Road-Side Unit (RSU) that can act as a centralized intersection manager and assign intersection crossing priorities. In the absence of RSU, there are some distributed CIM methods that only rely on communication among CAVs for situational awareness, however, none of them are specifically focused towards Stop Controlled-Intersection (SCI) with the aim of mitigating ambiguity among CAVs. Thus, we propose an Automated Right-of-Way (AROW) algorithm based on distributed CIM that is capable of reducing ambiguity and handling any level of non-compliance by CAVs. The algorithm is validated with extensive experiments for its functionality and robustness, and it outperforms the current solutions.

Index Terms—Cooperative Intersection Management, V2X, V2V, Right-of-Way, Stop-Controlled Intersections, Ambiguity

I. INTRODUCTION

INTERSECTION management is one of the most significant and challenging topics for safe and efficient driving experience. Intersections can be mainly divided into two categories, i.e., signalized and unsignalized intersections. Signalized intersections comprise of traffic lights, whereas the unsignalized intersections consists of stop or yield signs, or in some instances, no signs at all. The ever-increasing vehicles on roads can lead to congestion [1], traffic delays [2], and economic and societal costs due to crashes [3]. In this context, unsignalized [4] and signalized [5] intersections have been found to be hazardous and inefficient towards catering large volumes of traffic. Particularly, in unsignalized intersections, Stop Controlled-Intersections (SC-I) are a major source of crashes [4].

According to the United States National Motor Vehicle Causation Survey, around 35% of the crashes between 2005 and 2007 occurred on intersections, out of which, insufficient situational awareness and ambiguity over intersection priority

constituted for 44.1% and 8.4%, respectively [6]. Similarly, it was reported that in the United States and Europe, around 40% of all traffic accidents occurred at intersections [7]. Based on the National Highway Traffic Safety Administration (NHTSA) report [8] conducted in 2015, around 95% of the total vehicle crashes in the US from 2005 to 2007 were a consequence of human error, out of which, around 35% occurred due to bad driver decisions. Given these studies, it is critical to investigate intelligent traffic management systems.

In this regard, Cooperative Intersection Management (CIM) systems have been a major source of interest in the research community [9]–[11]. CIM systems are used by Connected and Autonomous Vehicles (CAVs) to improve the overall driver experience. CAVs employ Vehicle-to-Everything (V2X) communication [12]–[15] to enhance their situational awareness and improve safety standards while making driving decisions. Although there is abundant literature on CIM for signalized intersections [16]–[18], the focus of this study is on ambiguity mitigation at SC-I which is a subset of unsignalized intersections.

While numerous studies exist for unsignalized CIM in the space of cooperative resource reservation [19], trajectory planning [20], and collision avoidance [21], they are mostly dependent on a centralized Road-Side Unit (RSU) to function as an intersection manager for passing priorities and information about nearby CAVs [22], [23], thereby either partially or completely replacing the functionality of SC-Is. On the other hand, there is sparse literature on distributed CIM systems where CAVs solely rely on communication with each other without the presence of any RSU. Although there are some related works for SC-I in distributed CIM, none of the studies focus explicitly on resolving ambiguity among CAVs at SC-I.

VanMiddlesworth *et al.* [24] uses distributed CIM to navigate through SC-I, however, it is only feasible for a low number of CAVs. Secondly, although the authors discuss possible CAV non-compliance consideration, however, they do not provide a mechanism to test it and confirm the robustness of the system. The most related work is performed by Hassan *et al.* [25] where they present a distributed heuristic-based algorithm for cooperative SC-I management that outperforms the traditional First-in-First-Out (FIFO) approach at SC-I in terms of average delay, however, the study does not address ambiguity issues in cases when CAVs arrive at the SC-I at close intervals of each other. Also, the robustness of the algorithms is not tested under CAV non-compliance by CAVs.

Therefore, to address this, we propose a distributed CIM

¹ Connected & Autonomous Vehicle Research Lab (CAVREL), University of Central Florida, Orlando, FL, USA. gshah8@knights.ucf.edu

² Honda Research Institute, Ann Arbor, MI

algorithm namely Automated Right-of-Way (AROW) that utilizes an earlier designed and implemented Driver Messenger System (DMS) [26] based on the relevant source material [27]. CAVs can employ AROW in SC-I to negotiate SC-I crossing priorities and avoid any potential for ambiguity. The proposed algorithm is robust to any non-compliance from CAVs and not only assists in mitigating ambiguity, but also in promoting fairness when it comes to SC-I crossing, even for large-scale CAV scenarios.

II. DRIVER MESSENGER SYSTEM (DMS)

DMS allows CAVs to utilize sensor data and V2X communication to share application-specific Over-the-Air (OTA) Driver Intention Messages (DIMs) between Host Vehicle (HV) and Target Remote Vehicles (TVs). DMS is essentially divided into four main components which have been previously explained in detail by the authors [26]. Relevant details of these components specific to the application in focus are mentioned in the following.

A. Local Object Map

This is the first module within DMS and it creates and updates a local object map to localize the HV and the nearby RVs around it. For this paper, the authors only utilize GPS and V2X communication to create and update the local object map and localize the CAVs. It is assumed that all participating vehicles in any scenario are connected and that there are no communication losses due to congestion or bad resource allocation.

B. Application Detection

This module is tasked with utilizing the updated local object map and deciding if the HV is currently in one or more of the pre-defined applications within DMS. Once identified, DMS executes the corresponding application thread for the next application-specific tasks. In this study, we assume a four-way allway SC-I where each of the lanes connecting to the SC-I is a singular lane. However, the logic presented throughout in this study along with the proposed AROW algorithm can be applied to any kind of SC-I. Figure 1 shows an example of the SC-I used for this study.

Since only GPS and V2X communication in the form of Basic Safety Messages (BSMs) are utilized in the creation of the local object map, this study uses a pre-configured map setting with an SC-I whose location is already known by all the participating CAVs as ground-truth. Therefore, as CAVs approach the SC-I, they can utilize the known ground truth location of the SC-I to determine their distance ($dist$) from the SC-I and thus, the stop sign. The application detection block considers a CAV A to be within an SC-I application and trigger its application block as long as (1) below is satisfied:

$$dist_A \leq det_{thresh} \quad (1)$$

where $dist_A$ is the distance of A from the stop sign in its lane and det_{thresh} is the SC-I application detecting distance threshold. det_{thresh} is one of the configurable parameters of SC-I as explained in later sections.

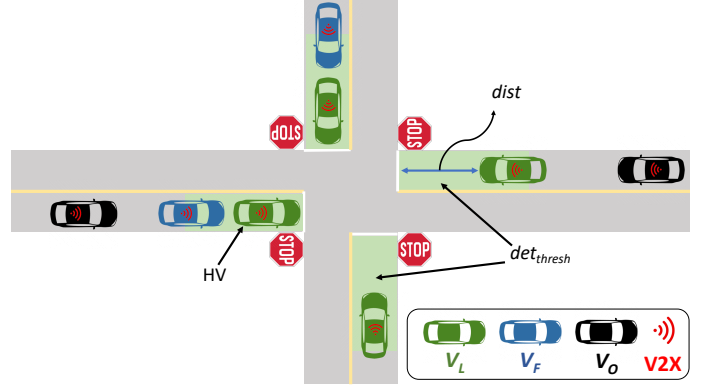


Fig. 1: Bird-eye view of a Stop Controlled-Intersection (SC-I) during application detection phase.

Another objective for any CAV within the application detection block upon approaching an SC-I is to detect whether it is the leading CAV in its lane to reach the stop sign or if it is following another CAV in front of it. As shown in Figure 1, a CAV A can be described in a typical SC-I scenario as shown in (2) below:

$$A = \begin{cases} v_L \in V_L & \text{if leading, } dist_A \leq det_{thresh} \\ v_F \in V_F & \text{if following, } dist_A \leq det_{thresh} \end{cases} \quad (2)$$

where v_L is the leading CAV in a particular lane while approaching an SC-I and it satisfies (1) and V_L is the current updated set of all leading CAVs in a SC-I. On the other hand, CAV v_F is following another CAV in front while approaching an SC-I while also satisfying (1) and V_F is the set of all following CAVs in an SC-I. Finally, CAV V_O may or may not be the leading CAV however it does not satisfy (1), and thus does not qualify for SC-I application. As explained in the next section, finding the state of a CAV and its proximity to an upcoming SC-I as per (2) is significant to determine its priority in the proposed AROW algorithm, especially in scenarios where there are queues of CAVs approaching an SC-I.

C. Application Block

Once the application detection block identifies that the HV is approaching an SC-I (1), DMS triggers the application execution block of SC-I. This block contains the proposed AROW algorithm whose main goal is to identify fellow CAVs at the SC-I through the local object map and negotiate SC-I crossing turns of all CAVs in consideration by a series of DIMs. It should be noted that all CAVs in this study are assumed to be equipped with DMS and thus the same AROW algorithm is going to be executed for all CAVs approaching an SC-I.

D. V2X Communication

This block is responsible for transmitting and receiving DIMs to and from the HV, respectively. DIMs are application-specific and their structure and content varies for every specific application within DMS. The details of DIM structure and

TABLE I: AROW DIMs and ACKs

| | |
|----------------------|---|
| AROW1 | SC-I introduction ($S1$) |
| AROW2 | V_{arb} announcement ($S2_2$) |
| ACK2 | Acknowledgment of AROW2 ($S2_3$) |
| AROW3 | V_{arb} turn scheduling ($S3_1$) |
| ACK3 | Acknowledgment of AROW3 ($S3_2$) |
| AROW4 ₁ | V_{arb} in-turn SC-I exit + assign new V_{arb} ($S4_1$) |
| AROW4 ₂ | In-turn SC-I exit ($S4_2$) |
| AROW5 | Out-of-turn SC-I exit ($S2_2, S2_3, S3_1, S3_2$) |
| AROW _{wait} | Request CAVs in V_S to wait for current AROW |

encoding/decoding procedures are not the focus of this paper and thus are not included.

III. AUTOMATED RIGHT-OF-WAY (AROW) ALGORITHM

AROW algorithm is executed inside the application module of SC-I within DMS where CAVs can utilize DIMs to assign priorities to cross an SC-I and reduce ambiguity. The SC-I application module within a HV is executed as soon as it satisfies (1) and it can be referred to as belonging to either V_L or V_F as per (2). On an abstract level, AROW considers the current total competing vehicles (V_T) at an SC-I such as that

$$n(V_T) = n(V_L) + n(V_F) \quad (3)$$

and it operates by assigning one of the V_L as the arbitrator CAV (V_{arb}) such that $V_{arb} \in V_L$ can assign priorities in the form of turns to all CAVs within V_L to avoid any ambiguity. One of the main contributions of AROW is that it is equipped to assign distinct crossing turns such that there is no duplicity and ambiguity. Secondly, it is also capable of countering situations where some participating CAVs in an SC-I scenario can turn out to be non-compliant with the rules of AROW and turns assigned by V_{arb} .

AROW comprises of several stages given the involved complexity and the task of maintaining resolution among multiple independent CAVs. Each stage within AROW involves transceiving of stage-specific DIMs and/or acknowledgment (ACK) signals as mentioned in Table I.

A. Stage 0 ($S0$) - Not in SC-I

This is the idle stage of AROW and the HV stays in this stage as long as it does not satisfy (1).

B. Stage 1 ($S1$) - SC-I Discovery

This is the first step in the execution of AROW where the HV satisfies (1) and broadcasts a discovery DIM known as AROW1. On a high-level, in addition to HV's basic safety and identification data, the contents of this DIM can be considered to highlight the detection of SC-I by the HV and the initiation of AROW algorithm within its DMS. Also, this DIM includes information pertaining to whether currently $HV \in V_L || HV \in V_F$. Just like the HV, any CAV starting its AROW process can be assumed to broadcast a similar AROW1 DIM. After broadcasting AROW1, the HV waits for a pre-configured timeout/clock-constraint $T1$ to receive any DIMs from other CAVs in V_T . The two types of receiving DIMs under focus in this stage are AROW1s from CAVs that have also just initiated AROW algorithm or AROW_{wait} from V_{arb} .

Towards the end of constraint $T1$, if the HV does not receive any DIM, then it can be considered that there are no fellow CAVs at the SC-I besides the HV itself. This triggers DMS to effectively terminate AROW and the HV is instructed by its DMS to cross the SC-I without AROW and switch to $S0$. On the other hand, if HV receives AROW1(s) from other CAVs but no AROW_{wait}, then this signifies that there is no V_{arb} present at SC-I but there are fellow competing CAVs that arrived at the SC-I at similar times as that of the HV, and that the AROW process should proceed into next stage, i.e. $S2_1$. Finally, if the HV receives AROW_{wait} from V_{arb} , this signals that there is a current AROW process going on where V_{arb} is arbitrating and negotiating SC-I crossing turns among a group of CAVs (V_P) that arrived at the SC-I at least $T1$ time before the HV. AROW_{wait} is sent by V_{arb} to any CAV A broadcasting AROW1 to signal it to wait for the current AROW process to end before A can participate for its own turn assignment. As detailed in the next sub-section, as soon as V_{arb} is assigned in $S2_1$ and until all its tasks in AROW are accomplished, V_{arb} maintains two updating sets in which it divides the CAVs from V_T such that:

- V_P : Set containing primary CAVs that are part of the current AROW procedure. These are always the leading CAVs.
- V_S : Set containing secondary CAVs that are instructed to wait for the current AROW procedure to finish before they can be considered for arbitration. These can either be following CAVs or leading CAVs that arrive during an ongoing AROW.

At any time within AROW, arbitration is always performed among CAVs that are present in V_P . Therefore, if HV receives AROW_{wait} from V_{arb} , then this indicates that HV needs to move to SW and wait for the current arbitration to end. In this case, HV is also added to V_S as it is not one of the CAVs considered for the current round of arbitration.

C. Stage 2₁ ($S2_1$) - V_{arb} Selection

In the case that HV receives at least one AROW1 from a fellow CAV but no AROW_{wait} from V_{arb} , AROW enters $S2_1$ in which a single CAV from V_L is chosen as V_{arb} for the remainder of the AROW process until V_{arb} crosses the SC-I on its assigned turn. Based on a fixed heuristic H_1 within DMS of every CAV in set V_L , one of the CAVs is chosen as V_{arb} . To ensure that all participating CAVs in V_L choose the same V_{arb} and there is no duplication, there is a single heuristic stored within DMS of all CAVs. For this study, the heuristic H_1 is as follows:

- H_1 : The last arriving CAV denoted from the timestamp at which it entered SC-I application by satisfying (1) and initiated its AROW, is chosen as V_{arb} . If two or more CAVs arrive at the same timestamp, then their unique CAV identification numbers can be utilized as tie breaker and the CAV with an alphanumeric character containing the lowest ASCII value at the first index with differing characters by process of elimination can be chosen as V_{arb} .

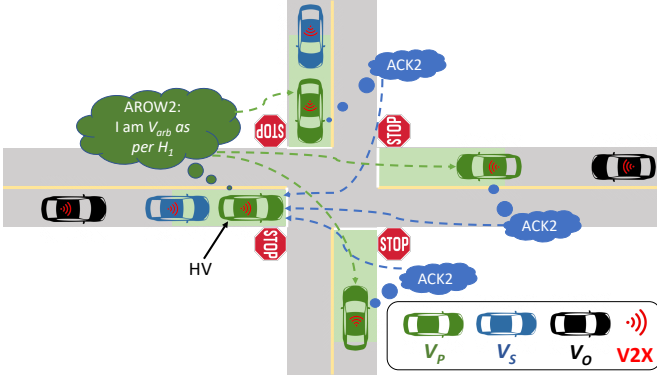


Fig. 2: Example scenario during HV's V_{arb} announcement in stage $S2_2$. HV had previously broadcasted its AROW2 DIM and the other competing CAVs in V_P are now sending their ACK2 signals.

Following this same H_1 , it can be guaranteed that all CAVs in V_L will choose the same CAV as V_{arb} .

Particular attention needs to be given to the fact that during this process of V_{arb} selection, only CAVs that are considered are the ones that were a part of V_L up until the end of clock $T1$. In other words, any new CAVs that entered the SC-I application after the current AROW process considering CAVs in V_L has already moved on from S_1 would not be considered in the current arbitration selection process even if it is now a part of V_L , since priority is given to CAVs that arrived at similar times in S_1 and have already passed to the next stage.

Whoever is chosen as the V_{arb} in this stage as per H_1 , the first task that it needs to perform is to divide up CAVs in V_T into V_P and V_S , as mentioned in the previous sub-section. All the CAVs as part of the current arbitrator process in $S2_1$ are included in V_P whereas all the CAVs in V_F are added to V_S . Also, if any CAV enters SC-I and its S_1 as a v_L or v_F while the current AROW process is going on in any stage after S_1 , it would be directly entered in set V_S by V_{arb} . At every timestamp throughout AROW, whenever any CAV enters or leaves SC-I, V_{arb} always updates both V_P and V_S .

Finally, during $S2_1$, if the HV is chosen to be the V_{arb} as per H_1 , then it goes into $S2_2$ and all the other CAVs in V_P proceed to their $S2_3$. On the other hand, if HV is not chosen to be the V_{arb} , then it proceeds to its $S2_3$ along with other CAVs in V_P that are also not chosen as V_{arb} whereas the CAV chosen as V_{arb} goes into $S2_2$.

D. Stage 2₂ ($S2_2$) - V_{arb} Announcement

In $S2_2$, the HV broadcasts AROW2 DIM in which it informs all the CAVs in V_P that it has been chosen as V_{arb} . After broadcasting AROW2, the HV waits for constraint $T2$ to receive acknowledgment signal ACK2 from CAVs in V_P as an acceptance of HV as V_{arb} . Figure 2 shows an example of AROW in $S2_2$ with HV as V_{arb} . After the completion of $T2$, if HV receives ACK2 from all V_P , then HV moves to $S3_1$, whereas the non-arbitrator CAVs in V_P move to $S3_2$. Alternatively, if there is non-compliance where one or more CAVs other than HV in V_P leave the SC-I prematurely, the other compliant CAVs in V_P along with any new CAVs in V_L that are not yet part of V_P can re-start AROW by

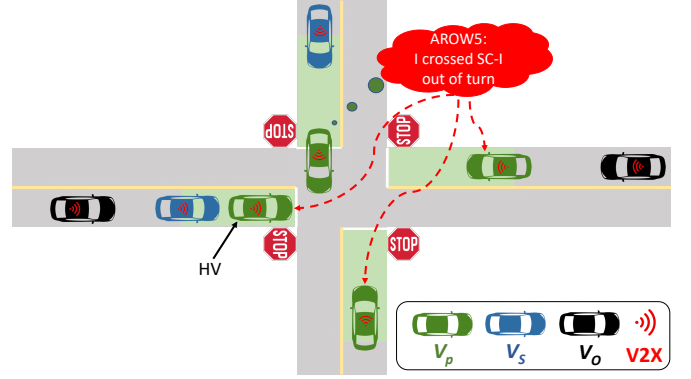


Fig. 3: Non-compliance scenario in AROW with HV as V_{arb} . One of the CAVs in V_P has become non-compliant and prematurely exited the SC-I upon which the DMS within it has broadcasted the AROW5 DIM.

going back to $S1$. The number of times the compliant CAVs can consecutively repeat a particular round of AROW in face of non-compliance is determined by the pre-configured $AROW_{thresh}$, as shown in the equation below:

$$AROW_{count} \leq AROW_{thresh} \quad (4)$$

where $AROW_{count}$ is the counter to keep track of the consecutive repetitions. As soon as (4) is not satisfied, DMS within all compliant CAVs in V_P switches to $S0$ and the CAVs can cross the SC-I manually without the assistance of AROW.

E. Stage 2₃ ($S2_3$) - V_{arb} Acceptance

In $S2_3$, since the HV is not chosen as V_{arb} , it waits for $T2$ to receive AROW2 DIM from V_{arb} , and upon reception, it needs to send an ACK2. Towards the end of $T2$, if all CAVs in V_P along with HV are compliant, then AROW moves HV into $S3_2$ along with other CAVs in V_P that are not V_{arb} . At the same time, AROW within V_{arb} moves it from $S2_2$ into $S3_1$ as explained in the previous subsection. However, if there is any non-compliance by a CAV in V_P or V_{arb} itself, then the AROW within HV and other compliant CAVs in V_P requires to break the current AROW process and move to either $S1$ or $S0$ depending on (4), as explained in the previous subsection.

F. Non-Compliance

Non-compliance is a condition within AROW that can occur when a CAV is in any of four stages defined as $NC_{stages} = \{S2_2, S2_3, S3_1, S3_2\}$. A CAV in V_P is said to be non-compliant whenever it crosses an SC-I prior to its assigned turn. Whenever it does, the out-of-turn CAV broadcasts an AROW5 exit DIM. This DIM is used by V_{arb} and other CAVs in V_P to identify a non-compliant CAV. Figure 3 shows an example of non-compliance where one of the CAVs in V_P decides to leave during $S2_2$ where turns have not even been assigned yet. As soon as AROW within that CAV detects the untimely exit, it broadcasts AROW5. Usually, DMS would utilize a camera to identify if it has already passed the SC-I to broadcast AROW5, however, since we only utilize V2X as the data source for this study, the ground truth data of the SC-I

is utilized for the purpose of identifying an exit from an SC-I and broadcasting AROW5 DIM. In this study, non-compliance can occur to any CAV in V_P during AROW including V_{arb} . The only exception to this is the HV itself. In other words, we always assume that the HV is always fully compliant. To evaluate the impact of non-compliance, it is probabilistically applied (NC_{prob}) to each CAV independently when it is in each of the four stages in NC_{stages} .

G. Stage 3₁ ($S3_1$) - Turn Scheduling

HV can arrive in $S3_1$ from either the parent stage $S2_2$ or SW . The details of switching from the former parent stage are explained later under the subsection of SW . In the case of parent stage $S2_2$, if the HV receives ACK2 signal from all CAVs in V_P after its selection as V_{arb} , HV moves into $S3_1$ while the other CAVs in V_P move to $S3_2$. This is the stage where the HV as V_{arb} assigns turns to all CAVs in V_P to cross the SC-I based on a fixed pre-configured heuristic H_2 . The main goal behind choosing any heuristic is to ensure that different turns are assigned to each CAV and that there is no duplication. The heuristic H_2 used for this study is defined as follows:

- H_2 : V_{arb} assigns turns based on the arrival timestamp of every CAV in V_P and prioritizes CAVs that arrived earlier at the SC-I. In the situation where more than one CAV carries identical arrival timestamp, V_{arb} can randomly assign turns among them.

The turn assignment information is enclosed within AROW DIM and broadcasted. Once received, the CAVs in V_P are required to reply with an ACK3 acknowledgment to confirm the corresponding turn assignment. After broadcasting AROW3, HV waits for constraint $T3$. Towards the end of $T3$, if the HV receives ACK3 signals from all relevant CAVs, then it moves towards $S4_1$. On the other hand, if there is non-compliance by any CAV, then depending on (4), HV either moves to $S1$ to restart AROW or to $S0$ where it disables AROW to manually pass the SC-I.

H. Stage 3₂ ($S3_2$) - Turn Acceptance

After passing $S2_3$, HV moves into $S3_2$ where, similar to that in $S2_3$, it waits for V_{arb} to send a AROW3 DIM that contains the turn assignment for the HV among other CAVs in V_P . Upon receiving AROW3, HV sends an ACK3 signal to acknowledge the reception. Once $T3$ is elapsed and there is no non-compliance, the HV moves into $S4_2$. However, just like in $S2_3$, if any CAV in V_P or V_{arb} becomes non-compliant, then HV moves into $S1$ or $S0$ depending on (4).

I. Stage 4₁ ($S4_1$) - Exit SC-I + Assign New V_{arb}

$S4_1$ is the ultimate stage for HV as V_{arb} in AROW. By the time the HV arrives in this stage and the other CAVs in V_P arrive in the corresponding $S4_2$, the turns have already been assigned to all involved CAVs along with the HV. HV stays in this stage until the arrival of its turn to cross the SC-I. Upon exiting the SC-I, the HV needs to perform one last task in its role as V_{arb} i.e. to choose a new V_{arb} as per a

pre-defined heuristic H_3 . For simplicity, this study uses H_1 as the heuristic for choosing new V_{arb} , i.e. ($H_3 = H_1$). If there are any CAVs in V_S waiting at the SC-I for the current AROW procedure involving HV and V_P to terminate, then HV as V_{arb} needs to select one of CAVs in V_S to become the new V_{arb} . After selecting new V_{arb} , HV crosses the SC-I, and broadcasts AROW4₁ DIM indicating to all other CAVs in V_T that it is exiting SC-I along with the information pertaining to new V_{arb} . Finally, AROW within HV moves to $S0$ as the idle stage.

J. Stage 4₂ ($S4_2$) - Exit SC-I

Similar to $S4_1$, HV waits for its turn to pass the SC-I. Once it does, it broadcasts a final AROW4₂ DIM, indicating to CAVs in V_T that it is leaving the SC-I, and then its AROW moves to $S0$.

K. Stage Wait (SW) - Wait for current AROW completion

If HV arrives at SC-I by satisfying (1) with an ongoing AROW arbitration round, then the V_{arb} instructs HV via AROW_{wait} to wait in SW as one of V_S . If the current AROW concludes successfully without any non-compliance, then depending on the set V_S , the HV can either move to $S0$, $S3_1$, or $S3_2$. If HV is the only CAV in V_S , then AROW is not required and HV can manually pass the SC-I, thus HV moves to $S0$. In the case of presence of other CAVs in V_S , HV can move to $S3_1$ if V_{arb} of the concluding AROW has chosen HV to be the new V_{arb} via AROW4₁ DIM, otherwise, it transitions to $S3_2$. The process of assigning new V_{arb} assists in optimizing AROW since it avoids the need for CAVs to utilize AROW from the beginning stage of $S1$. Finally, if there is non-compliance among competing CAVs in V_P while HV is in SW and (4) is not satisfied which means that all CAVs in V_P collectively eliminate AROW and manually pass SC-I, then HV along with others CAVs in V_S move to $S1$ to initiate AROW from the beginning.

IV. AROW IMPLEMENTATION AS A TIMED AUTOMATON

This section provides details into the earlier-introduced stages within AROW and shows their functionality as distinguishable states. AROW can be modeled as a timed automaton [28], [29] that allows it to be within a particular state at any specific time due to timing constraints. Figure 4 represents AROW as a timed automaton. The automaton consists of nodes called locations and edges known as switches. Formally, the automaton can be described as a tuple $\mathcal{M} = \langle S, S^0, A, X, I, E \rangle$ where

- S is a finite set of all locations within \mathcal{M} and it can be defined as

$$S = \{SW, S0, S1, S2_1, S2_2, S2_3, S3_1, S3_2, S4_1, S4_2\} \quad (5)$$

Each location in S defines a particular AROW stage which has been explained in detail in the previous section. Figure 4 provides a description highlight for each location.

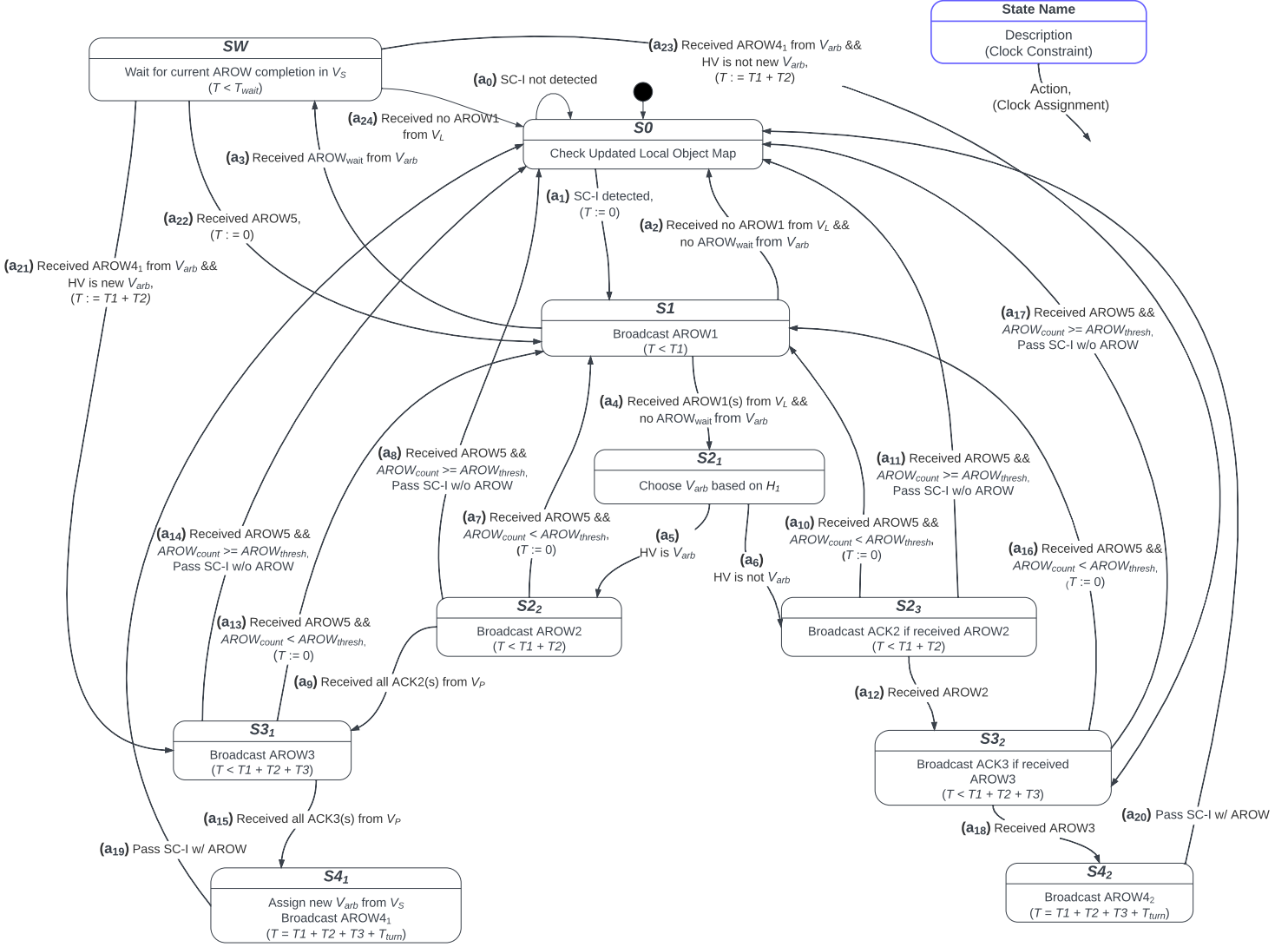


Fig. 4: AROW algorithm expressed as a timed automaton

- $S^0 \subseteq S$ is a set of initial locations. For AROW system,

$$S^0 = \{S0\} \quad (6)$$

This is also the location where AROW is typically deactivated which means that whenever HV is in this location, it is not approaching a nearby SC-I.

- A is a finite set of input symbols,

$$A = \{a_i \mid i \in \mathbb{N}, 0 \leq i \leq 24\} \quad (7)$$

This signifies that the total number of symbols in AROW are equal to 24.

- X is a finite set of clocks. The transition system for AROW only utilizes a singular clock T ,

$$X = \{T\} \quad (8)$$

- I is a mapping that assigns locations within \mathcal{M} with clock constraints in set $\Phi(X)$. Given that (8) contains only a

singular clock, all the constraints in $\Phi(X)$ are defined for T ,

$$\Phi(X) = \{T_1, T_1 + T_2, T_1 + T_2 + T_3, T_1 + T_2 + T_3 + T_{turn}, T_{wait}\} \quad (9)$$

These constraints are included in specific locations within the description blocks as observable in Figure 4. I maps these constraints from $\Phi(X)$ for clock T on select locations within \mathcal{M} as mentioned below:

- $S1 : T < T_1$
- $S22, S23 : T < T_1 + T_2$
- $S31, S32 : T < T_1 + T_2 + T_3$
- $S41, S42 : T < T_1 + T_2 + T_3 + T_{turn}$
- $SW : T < T_{wait}$

All locations within \mathcal{M} not mentioned in the mapping above can be considered as not possessing any clock constraint.

- $E \subseteq S \times A \times 2^X \times \Phi(X) \times S$ is a set of switches between locations within \mathcal{M} . A switch $\langle s, a, \varphi, \lambda, s' \rangle$ repre-

TABLE II: SUMO simulation parameters

| | |
|-----------------------------------|---------------------|
| Experiment Duration | 5000s |
| No. of CAVs (n_{veh}) | 4, 8, 16 |
| Car-Following Model | Krauss [30] |
| Maximum Vehicle Speed | 70 m/s |
| Vehicle Acceleration | 2.6m/s ² |
| Vehicle Deceleration | 4.5m/s ² |
| Sigma (Driver Imperfection) | 0.5 |
| minGap (Empty space after leader) | 2.5m |
| CAV length | 5m |
| Road Topology | Circled Plus |
| No. of lanes/road segment | 1 |

sents a transition edge from location s to s' over a symbol a . A switch can also comprise of a timing constraint φ over X that specifies when the transition switch can be used. Also, a switch can also contain the set $\lambda \subseteq X$ that allows clocks to be reset to a particular value with this switch.

It should be noted that none of the switches in E have clock constraint φ over X . In other words, none of the switches in AROW system require fulfillment of clock constraint to be executed for a location switch to occur. However, there exist some switches within \mathcal{M} in which the clock T is reset. Since X only contains a single clock T throughout \mathcal{M} , therefore λ also only comprises of X , i.e.

$$\lambda = \{T\} \quad (10)$$

All such instances are mentioned below where $e_i \subseteq E$ switches contain a clock T reset:

- $e_1, e_7, e_{10}, e_{13}, e_{16}, e_{22} : T = 0$
- $e_{21}, e_{23} : T = T1 + T2$

Every i in e_i mentioned above corresponds to the switch containing an input symbol $a_i \in A$ as in (7).

N is the transition system of \mathcal{M} . State of N can be described as a pair (s, v) where $s \in S$ denotes the current location and v represents the clock interpretation for X as in (8) such that v satisfies the constraint of the clock mapped to s by $I(s)$. A transition $N_p \in N$ can be described in two ways:

- In the case of self-transition where a transition state returns to itself due to clock constraint,

$$N_p : (s_i, v) \xrightarrow{\delta} (s_i, v + \delta), \quad (11)$$

where the clock increment δ is such that $v + \delta$ satisfies the clock constraint set by $I(s_i)$ mapping. Also, the source and destination location is s_i signifying the self-transition.

- In the case of transition switch from one location s_i to another s_j based on $e \in E$,

$$N_p : (s_i, v) \xrightarrow{a} (s_j, v[\lambda := y]), \quad (12)$$

where v satisfies φ , and a is part of the the transition edge e . Also, s_i and s_j are the source and destination locations, respectively. y represents the reset of the clock upon reaching the destination location.

As afore-mentioned, there are multiple reset values set up for the clock T in different locations along with some locations

TABLE III: AROW configurable parameters

| | |
|-------------------------------|------------------|
| det_{thresh} | 10m |
| BSM Periodicity | {100,600}ms [33] |
| Resource Reservation Interval | 100ms [34] |
| $T1$ | 2s |
| $T2$ | 2s |
| $T3$ | 2s |
| Non-Compliance Probability | 0, 0.1, 0.25 |
| $AROW_{thresh}$ | 2 |

that do not contain any particular reset. Thus, for simplicity, $v[\lambda := y]$ will just referred to as v' for this study and the clock constraints for each transition will not be explicitly mentioned as they can be clearly observed in Figure 4. This transition system will be repeatedly utilized for analysis in the next sections. The focus will be on transitions caused by location switches and will generally be mentioned as $N_t : (s_i, v) \xrightarrow{a_t} (s_j, v')$, where a_t refers to symbols in \mathcal{M} as shown in Figure 4 and satisfy (7).

V. EXPERIMENTAL RESULTS

A. Simulation and AROW Configuration Parameters

To test AROW and provide experimental details regarding its functionality, the transition system \mathcal{M} defined in the last section is modeled and tested using the Simulation of Urban Mobility (SUMO) traffic simulator [31]. The simulation parameters specific to SUMO are mentioned in Table II. These parameters can be configured as per user preference. The road topology used for this study considers a four-way allway SC-I attached to four single-lane road segments. Each end of the four road segments from SC-I is about 51.2m in length and connected to a circular round-about to facilitate CAVs to drive in an endless loop and repeatedly pass through the SC-I in the center for the entirety of the simulation. In order for the AROW algorithm to interact in real-time with SUMO simulation, the authors utilize Traffic Control Interface (TraCI) [32]. To test a variety of use-cases, the study utilizes different number of CAVs, i.e. $n_{veh} = 4, 8$, or 16 . Given the road topology, these values of n_{veh} can be considered as low, medium, and high density traffic, respectively.

Table III shows the values assigned to the configurable parameters of AROW for this study. The det_{thresh} is chosen to be 10m with aim to: (i) allow the CAVs to initiate the process of AROW in advance so that generally the CAV is assigned its turn to leave SC-I by the time it arrives at the stop sign, provided there is no non-compliance, and (ii) to allow up to two CAVs per lane to be included in the AROW process given the CAV length mentioned in Table II. On the other hand, $AROW_{thresh} = 2$ to provide compliant CAVs with at most two consecutive chances to use AROW to eliminate ambiguity in the face of non-compliance. $AROW_{thresh}$ should not be set to a really high value since it can then unfairly penalize compliant CAVs for following AROW rules since they will end up spending more time waiting to pass the SC-I.

As explained earlier, $T1$ is the timeout clock used by a CAV during discovery stage $S1$ of AROW. $T1$ for this study is set to 2s to allow realistic chance for one or more CAVs to initiate AROW and these CAVs can then enter in an arbitration

as mentioned in the AROW logic explained in the previous sections. T_2 is the timeout clock used to control how long a CAV stays in S_{2_2} or S_{2_3} while undergoing AROW process. The experimental value of T_2 is chosen to be 2s for CAVs in S_{2_2} and S_{2_3} . The realistic duration for T_2 can be further reduced and optimized based on the inherent communication latencies of the V2X technology in use. This optimization is the subject of a future study related to this topic. The same logic is applied to choosing the duration for T_3 .

B. Analysis and Results

1) *AROW Performance under Full Compliance* ($NC_{prob} = 0$): The first goal using simulations is to prove the completeness of the logic of AROW. To achieve this, the simulations using AROW with parameters mentioned in Tables II and III are run and each state's frequency and transitions are independently logged throughout the simulation duration. It should be noted that the terms 'state frequency' and 'state transitions' are used instead of 'location frequency' and 'location transition' to specify that these values have been collected over time in a simulation whenever the clock constraints for each transition are fulfilled as mentioned earlier in the description of the timed automaton \mathcal{M} of AROW. For this set of simulations, all the participating CAVs are set to be fully compliant, i.e. $NC_{prob} = 0$. The results of these simulations are shown in Figure 5 and Table IV. Figure 5 shows the state transitions matrices represented as heat maps and based on the transition system N of AROW. The x-axis and y-axis denote the destination and source locations, respectively. In addition to Figure 5, Table IV provides the state frequency in terms of raw numbers and percentages for each location.

For each of the three simulations, Table IV shows state frequency of each location and the transition matrix provides the outgoing and incoming transition switches from that location, respectively. For example, for $n_{veh} = 4$, S_{3_1} has a percentage frequency of 3.98% and the transition matrix clarifies this frequency by showing that S_{3_1} has two incoming transition switches $N_{21} : (SW, v) \xrightarrow{a_{21}} (S_{3_1}, v')$, and $N_9 : (S_{2_2}, v) \xrightarrow{a_9} (S_{3_1}, v')$ with frequencies of 1.53% and 2.45%, respectively, that add up to 3.98%, equal to state frequency of S_{3_1} as shown in Table IV. Additionally, the transition matrix also shows one outgoing transition switch from S_{3_1} , i.e. $N_{15} : (S_{3_1}, v) \xrightarrow{a_{15}} (S_{4_1}, v')$ worth 3.98% which is again equal to the incoming transitions to S_{3_1} and also its percentage frequency. The equality between incoming and outgoing transition switches can be observed for all locations in all traffic scenarios, except for minuscule differences due

TABLE IV: Raw state frequencies from simulations in Figure 5 with full compliance ($NC_{prob} = 0$)

| n_{veh} | SW | S0 | S1 | S2 ₁ | S2 ₂ | S2 ₃ | S3 ₁ | S3 ₂ | S4 ₁ | S4 ₂ | Total |
|-----------|-------|-------|-------|-----------------|-----------------|-----------------|-----------------|-----------------|-----------------|-----------------|-------|
| 4 | 814 | 1577 | 1577 | 256 | 130 | 126 | 211 | 201 | 211 | 201 | 5304 |
| | 15.35 | 29.73 | 29.73 | 4.83 | 2.45 | 2.38 | 3.98 | 3.79 | 3.98 | 3.79 | 100% |
| 8 | 1146 | 1159 | 1159 | 12 | 4 | 8 | 400 | 675 | 400 | 675 | 5638 |
| | 20.33 | 20.56 | 20.56 | 0.21 | 0.07 | 0.14 | 7.09 | 11.97 | 7.09 | 11.97 | 100% |
| 16 | 587 | 588 | 588 | 1 | 0 | 1 | 167 | 421 | 167 | 421 | 2941 |
| | 19.96 | 19.99 | 19.99 | 0.03 | 0 | 0.03 | 5.68 | 14.31 | 5.68 | 14.31 | 100% |

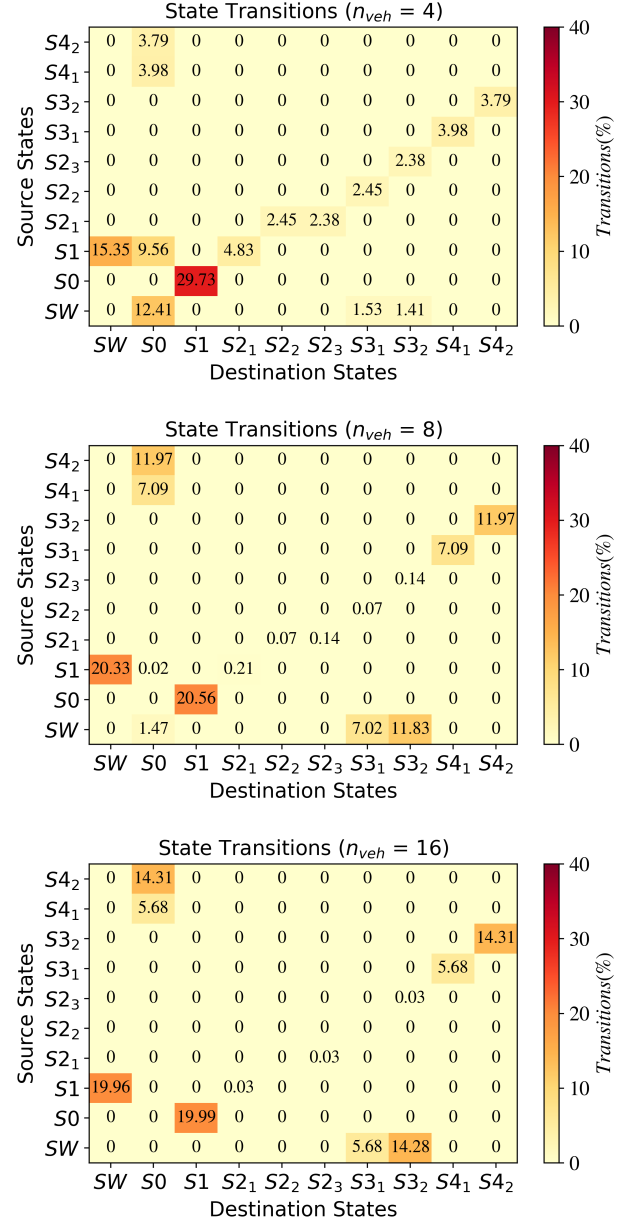


Fig. 5: State transition comparison for simulations with full compliance ($NC_{prob} = 0$)

to rounding in percentages. All the transitions in the matrices can also be observed to be in line with those in the timed automaton \mathcal{M} and use switches E corresponding to input symbols A in Figure 4, thereby ensuring that the experimental operation is corresponding to the AROW theory. Finally, all transitions within each matrix along with the state frequency percentages in Table IV add up to 100%, barring rounding errors.

Comparing the three simulations, it can be first observed that as the value of n_{veh} increases from 4 to 8, the total raw frequency increases by a small margin as shown in Table IV. This is mainly due to the fact that this higher number of CAVs in the scenario increases the frequency of HV's transition to SW upon its arrival at the SC-I in focus. Furthermore, as

n_{veh} increases to 16, there is a sharp reduction in the total raw frequency which is caused by a reduction in the count of S_0 and S_1 . This is mainly because as n_{veh} increases, there is a higher congestion at the SC-I in focus. Thus, the HV spends more time to get through SC-I and hence, fewer transitions switches of $N_1 : (S_0, v) \xrightarrow{a_1} (S_1, v')$ from S_0 to S_1 in the given simulation duration. The percentage equality of S_0 and S_1 in every simulation also attests to the 100% N_1 transition from S_0 to S_1 as shown in the graph \mathcal{M} in Figure 4.

From S_1 , the transition $N_2 : (S_1, v) \xrightarrow{a_2} (S_0, v')$ to S_0 occurs when the HV is unaccompanied by any fellow competing CAV at the SC-I, and in this case, the HV passes SC-I without AROW. As expected, the matrix for $n_{veh} = 4$ shows N_1 transition frequency of 9.56%, which goes to almost 0% in the case of $n_{veh} = 8, 16$ since with more CAVs, there is a lesser probability of HV approaching the SC-I in focus without any competition. On the other hand, the transition $N_3 : (S_1, v) \xrightarrow{a_3} (SW, v')$ to SW occurs when HV initiates AROW in the middle of an ongoing AROW round among CAVs in V_P . In this case, V_{arb} instructs HV to wait in SW . It can be seen in both the percentage state frequency and matrices that the frequency of N_3 is higher for $n_{veh} = 8, 16$ because as n_{veh} increases, there is a higher probability that HV would arrive at SC-I in focus and initiate in the presence of other CAVs.

One more transition possibility from S_1 is $N_4 : (S_1, v) \xrightarrow{a_4} (S_{21}, v')$ to S_{21} . N_4 occurs when HV is accompanied by other competing CAVs in V_L in SC-I and there is no V_{arb} present. In this case, the CAVs along with HV need to follow AROW and elect a V_{arb} . Again, as n_{veh} increases, there is a higher probability of a V_{arb} already present upon the arrival of HV, thus the frequency of N_4 reduces. This is why N_4 frequency for $n_{veh} = 4$ is 4.83% whereas it drops to just 0.21% and 0.03% for $n_{veh} = 8$ and $n_{veh} = 16$, respectively. From S_{21} , the only transitions are $N_5 : (S_{21}, v) \xrightarrow{a_5} (S_{22}, v')$ and $N_6 : (S_{21}, v) \xrightarrow{a_6} (S_{23}, v')$ to S_{22} and S_{23} , respectively. These transitions can be seen in the transition matrices and for the same afore-mentioned reason of a higher frequency of N_4 for $n_{veh} = 4$, we can also observe a higher frequency of N_5 and N_6 for $n_{veh} = 4$ that sum to the total state frequency of N_4 . Similarly, the transitions from S_{22} and S_{23} are $N_9 : (S_{22}, v) \xrightarrow{a_9} (S_{31}, v')$, and $N_{12} : (S_{23}, v) \xrightarrow{a_{12}} (S_{32}, v')$ to S_{31} and S_{32} , respectively, and carry a higher frequency in the case of $n_{veh} = 4$ as compared to other scenarios. It should be noted that since $NC_{prob} = 0$ in this set of three simulations, the transitions $N_8 : (S_{22}, v) \xrightarrow{a_8} (S_0, v')$, $N_7 : (S_{22}, v) \xrightarrow{a_7} (S_1, v')$, $N_{11} : (S_{23}, v) \xrightarrow{a_{11}} (S_0, v')$, $N_{10} : (S_{23}, v) \xrightarrow{a_{10}} (S_1, v')$ are all 0%.

For SW , the transitions are $N_{24} : (SW, v) \xrightarrow{a_{24}} (S_0, v')$, $N_{22} : (SW, v) \xrightarrow{a_{22}} (S_1, v')$, $N_{21} : (SW, v) \xrightarrow{a_{21}} (S_{31}, v')$, and $N_{23} : (SW, v) \xrightarrow{a_{23}} (S_{32}, v')$ to S_0 , S_1 , S_{31} , and S_{32} , respectively. N_{24} occurs in the cases when HV is ready to switch from SW upon the conclusion of current AROW round of other CAVs in V_P , however, there is no other waiting CAV besides HV, thus AROW is not required for HV. As expected, this transition majorly occurs in $n_{veh} = 4$ scenario with less CAVs (12.41%), and the other scenarios with higher CAVs,

the frequency of N_{24} reduces rapidly. The transition N_{22} is 0% for all scenarios here since all CAVs are fully compliant ($NC_{prob} = 0$). The transitions N_{21} and N_{23} occur in the cases when HV, along with other waiting CAVs in V_S is ready to switch out from SW upon the conclusion of the current AROW round and the V_{arb} has chosen on the CAVs from V_P to become the new V_{arb} . If HV is chosen as the new V_{arb} , then it follows N_{21} , otherwise it uses N_{23} as per AROW rules. As shown in the Figure 5 transition matrices, these transitions contain higher frequencies as n_{veh} increases, simply due to the earlier-stated argument that a higher number of competing CAVs creates a higher probability of CAVs in SW .

Finally, from S_{31} and S_{32} , the only valid transitions in the case of $NC_{prob} = 0$ are $N_{15} : (S_{31}, v) \xrightarrow{a_{15}} (S_{41}, v')$ and $N_{18} : (S_{32}, v) \xrightarrow{a_{18}} (S_{42}, v')$, respectively. For the same reason, the transitions $N_{13} : (S_{31}, v) \xrightarrow{a_{13}} (S_1, v')$, $N_{14} : (S_{31}, v) \xrightarrow{a_{14}} (S_0, v')$, $N_{16} : (S_{32}, v) \xrightarrow{a_{16}} (S_1, v')$, $N_{17} : (S_{32}, v) \xrightarrow{a_{17}} (S_0, v')$ are 0%. With the increase of n_{veh} , there are more instances of competing CAVs with HV, and thus the percentage of N_{15} and N_{18} also rises. Once CAVs successfully conclude AROW in S_{41} or S_{42} , AROW is transitioned back to S_0 using transitions $N_{19} : (S_{41}, v) \xrightarrow{a_{19}} (S_0, v')$ and $N_{20} : (S_{42}, v) \xrightarrow{a_{20}} (S_0, v')$, respectively.

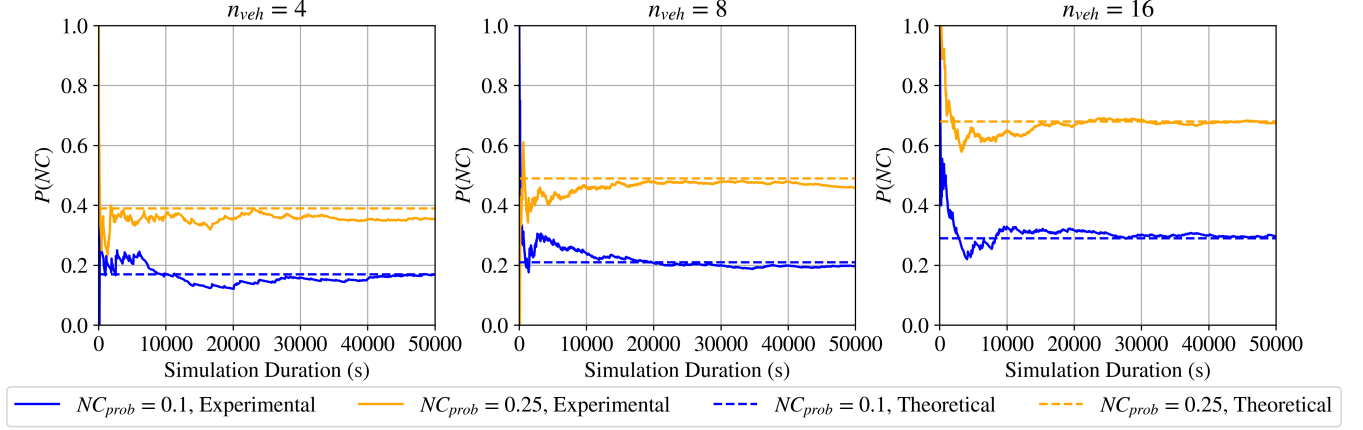
2) AROW Performance under Non-Compliance Scenarios:

a) *Theoretical analysis of Non-Compliance:* To increase robustness, AROW considers the occurrence of non-compliance and allows compliant CAVs to still reduce ambiguity and safely pass SC-I. To show the impact of non-compliance, this study randomly assigns non-compliance probability, i.e., NC_{prob} , to each CAV except HV every time they engage in AROW. There are two values used for experimentation purposes, i.e. $NC_{prob} = 0.1$, or 0.25. Even higher values can be chosen, but for the purposes of this paper, these values are sufficient to show the collective impact of NC_{prob} on AROW. In theory, NC_{prob} is designed to be independently applied to each CAV during each of the stages in NC_{stages} .

To show the collective impact of NC_{prob} on a typical round of AROW, we use a metric $P(\exists NC)$ which is the probability that at least one CAV becomes non-compliant throughout a singular round of AROW. Using the law of total probability $P(X) = \sum_n P(X \cap Y_n)$, we calculate $P(\exists NC)$ below:

$$P(\exists NC) = \sum_j^{n_{CV}} \sum_m^j \sum_i^{NC_{stages}} P(HV_i)P(NC_m|HV_i)P(CV_j), \quad (13)$$

where $P(HV_i)$ is the probability that HV is in stage i , $P(NC_m|HV_i)$ is the conditional probability that there are m non-compliant CAVs when HV is in stage i , and $P(CV_j)$ is the probability of HV in the current AROW round with j competing CAVs. $P(CV_j)$ uses the outermost sum where $CV \in V_P$ and n_{CV} is the total number of competing CAVs to the HV during a singular round of AROW. Considering the experimental topology for this study where competing CAVs can be on any of the single-lane roads of the SC-I, n_{CV} can be ranged as $1 \leq j \leq 3$. For every j in the outermost sum, the inner sum aggregates $P(NC_m|HV_i)$ in

Fig. 6: Comparison between $P_T(\exists NC)$ and $P_E(\exists NC)$

range $1 \leq m \leq j$. Finally, over every m , the inner-most sum aggregates $P(HV_i)$ where i is every location defined in NC_{stages} , i.e. $NC_{stages} = \{S2_2, S2_3, S3_1, S3_2\}$. As can be observed in (13), the probability $P(\exists NC)$ is calculated from the perspective of the HV due to the easiness of calculations. For example, if HV is in $S2_2$, we can already infer that other CAVs in V_P will be in $S2_3$, or if HV is in $S2_3$, we can then infer that one of the CAVs in V_P other than HV has been chosen as V_{arb} and has proceeded to $S2_2$, whereas remaining CAVs have moved to $S2_3$ along with HV. The same logic can be applied for HV being in $S3_1$ or $S3_2$.

$P(CV_j)$ is non-deterministic since it is not possible to predict the specific number of competing CAVs to HV at a specific time, and thus in this experiment, we rely on simulations to estimate it. On the other hand, when calculating probability $P(NC_m|HV_i)$ and given the set NC_{stages} , it can be observed that $P(NC_m|HV_{S2_2}) = P(NC_m|HV_{S2_3})$ and similarly, $P(NC_m|HV_{S3_1}) = P(NC_m|HV_{S3_2})$. On a high-level, $P(NC_m|HV_i)$ can be defined as:

$$P(NC_m|HV_i) = \binom{j}{m} * P(NC|HV_i)^m * (1 - P(NC|HV_i))^{(j-m)} \quad (14)$$

where $\binom{j}{m} = \frac{j!}{m!(j-m)!}$ is the binomial coefficient representing the different combinations of m non-compliant CAVs, $P(NC|HV_i) = NC_{prob}$, $P(NC|HV_i)^m$ is the probability of m non-compliant CAVs, and $(1 - P(NC|HV_i))^{(j-m)}$ is the probability of $(j-m)$ CAVs being compliant. Finally, $P(HV_i)$ is calculated as:

$$P(HV_i) = \begin{cases} (P(N_4^*) + P(N_3)P(N_{22})P(N_4^+))P(N_5) & \text{if } i = S2_2, \\ (P(N_4^*) + P(N_3)P(N_{22})P(N_4^+))P(N_6) & \text{if } i = S2_3, \\ P(HV_{S2_2})P_C(S2_2) + P(N_3)P(N_{21}) & \text{if } i = S3_1, \\ P(HV_{S2_3})P_C(S2_3) + P(N_3)P(N_{22}) & \text{if } i = S3_2 \end{cases} \quad (15)$$

where

$$P_C(t) = (1 - P(NC|HV_t))^j \quad (16)$$

As observable in (15), $P(HV_i)$ yields different values depending on the specific location and its parent locations. For

| n_{veh} | NC_{prob} | $P_T(\exists NC)$ | $P_E(\exists NC)$ |
|-----------|-------------|-------------------|-------------------|
| 4 | 0.1 | 0.17 | 0.17 |
| | 0.25 | 0.39 | 0.35 |
| 8 | 0.1 | 0.21 | 0.2 |
| | 0.25 | 0.49 | 0.46 |
| 16 | 0.1 | 0.29 | 0.29 |
| | 0.25 | 0.68 | 0.68 |

TABLE V: Tabular comparison between $P_T(\exists NC)$ and $P_E(\exists NC)$

instance, $P(HV_{S2_2})$ or the probability that HV arrives in $S2_2$ is dependent on either the direct transition $N_4^* : (S1, v) \xrightarrow{a_4} (S2_1, v')$ or sequence of transitions $N_3 : (S1, v) \xrightarrow{a_3} (SW, v')$, $N_{22} : (SW, v) \xrightarrow{a_{22}} (S1, v')$, and $N_4^+ : (S1, v) \xrightarrow{a_4} (S2_1, v')$. After considering the possibilities of HV arriving at $S2_1$, the result is multiplied by $P(N_5)$ to calculate $P(HV_{S2_2})$ where $N_5 : (S2_1, v) \xrightarrow{a_5} (S2_2, v')$. It should be noted that $\|N_4\| = \|N_4^*\| + \|N_4^+\|$, and these transitions are separated out due to probability calculations. $P(HV_{S2_3})$ is also similarly calculated for HV in $S2_3$. Calculating $P(HV_{S3_1})$ and $P(HV_{S3_2})$ is comparatively more complex because in addition to arriving at $S3_1$ or $S3_2$ from $S2_2$ or $S2_3$ using transitions $N_9 : (S2_2, v) \xrightarrow{a_9} (S3_1, v')$ or $N_{12} : (S2_3, v) \xrightarrow{a_{12}} (S3_2, v')$, respectively, HV can also arrive at $S3_1$ or $S3_2$ from the wait stage SW using transitions $N_{21} : (SW, v) \xrightarrow{a_{21}} (S3_1, v')$ or $N_{23} : (SW, v) \xrightarrow{a_{23}} (S3_2, v')$, respectively. In addition, in the cases of HV arriving at $S3_1$ or $S3_2$ from $S2_2$ or $S2_3$, it is also necessary for all competing CAVs to HV to be compliant in the parent locations $S2_2$ or $S2_3$, respectively. This can be calculated probabilistically using (16).

Given j which is the number of competing CAVs to HV in the current iteration of (13), some probabilities in (15) such as $P(N_5)$, $P(N_6)$, $P(N_{21})$, and $P(N_{23})$ can be determined probabilistically, whereas other remaining probabilities such as $P(N_4^*)$, $P(N_4^+)$, $P(N_3)$, $P(N_{22})$ are non-deterministic since they totally depend on the particular scenario. Finally, since we are calculating $P(\exists NC)$ where it is assumed that $1 \leq n_{CV} \leq 3$, thus $P(N_4^+)$ is always assumed to be 1.

b) *Experimental Analysis of Non-Compliance*: Given the parameters in Tables II and III and (13), (14), (15), and (16), we run a total of six simulations using different values of n_{veh} and NC_{prob} and compare the theoretical and experi-

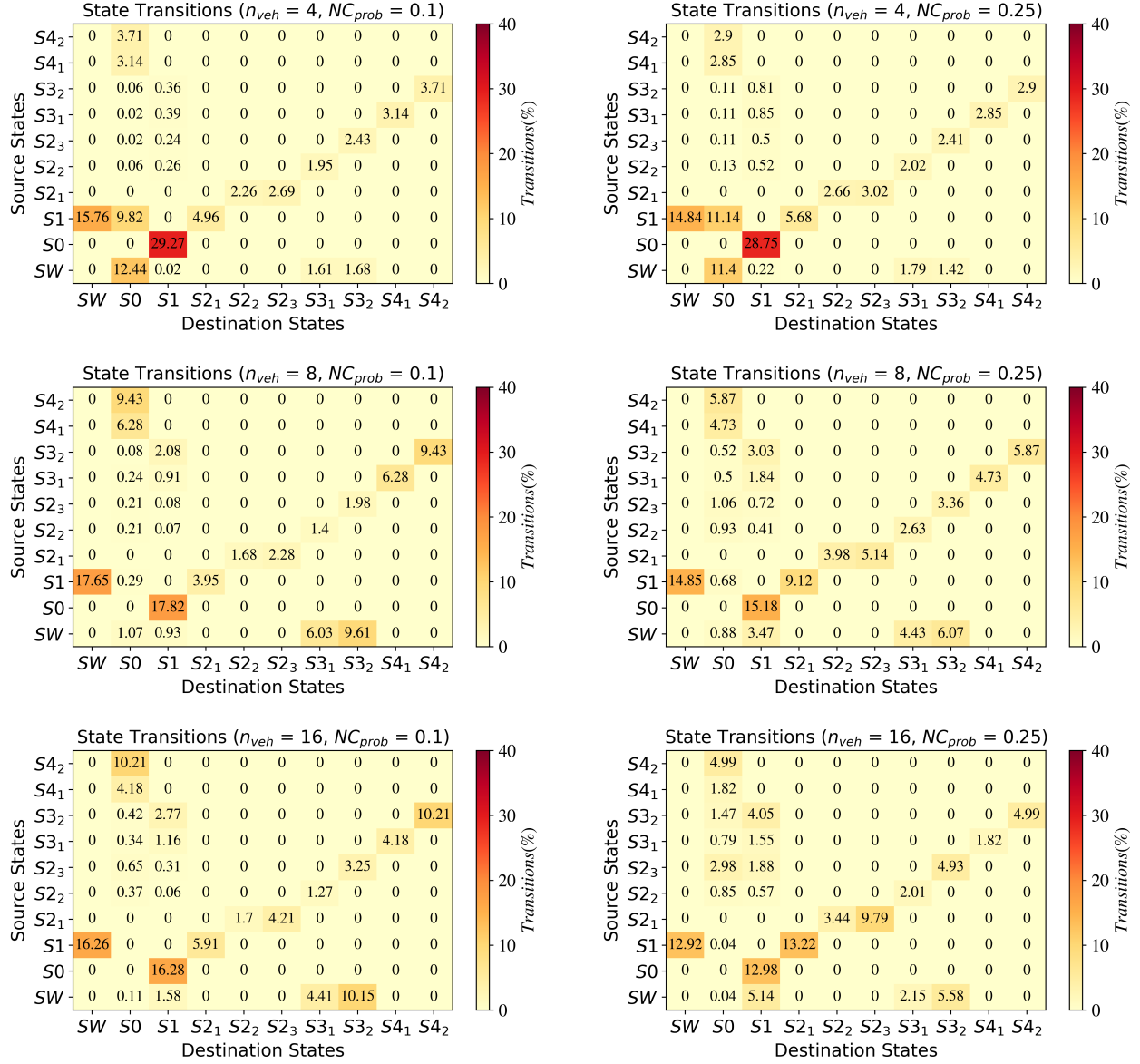


Fig. 7: State transition comparison for non-compliance scenarios ($NC_{prob} = 0.1$, $NC_{prob} = 0.25$)

mental $P(\exists NC)$, i.e. $P_E(\exists NC)$ and $P_T(\exists NC)$, as shown in Figure 6. It should be noted that the earlier-mentioned non-deterministic probabilities that are needed to calculate $P_T(\exists NC)$ are taken from the simulations for each scenario as known probabilities. As observable in all simulation results in Figure 6, $P_E(\exists NC)$ converges to $P_T(\exists NC)$ as the simulation moves ahead in time, which proves that AROW correctly considers the impact of NC_{prob} and the experimental results match with that of the theoretical concept. This also shows that the simulation duration and logging data size are sufficient to validate that the AROW algorithm has no deadlocks among a variation of scenarios. Table V points to the same convergence in tabular form as $P_T(\exists NC)$ and $P_E(\exists NC)$ are very similar to each other towards the end of the simulation duration. For all simulation scenarios, it can be generally viewed that as expected, an increase in NC_{prob} results in an

increase in the overall $P_T(\exists NC)$ and $P_E(\exists NC)$. Secondly, an increase in n_{veh} also increases $P_T(\exists NC)$ and $P_E(\exists NC)$ for both values of NC_{prob} since more n_{veh} results in more competing CAVs with HV during every AROW round. As evident from Table VI, as we increase n_{veh} for both values of NC_{prob} , the percentage of AROW rounds involving HV with a higher number of competing CAVs rises. For instance, with simulations scenarios where $n_{veh} = 4$, the highest percentage of AROW rounds for HV are with 1 competing CAV. For $n_{veh} = 8, 16$, the highest percentage changes to 2 and 3 competing CAVs, respectively. Therefore, this explains why $P_T(\exists NC)$ and $P_E(\exists NC)$ increase with the increase in n_{veh} .

After establishing the fact that the theoretical impact of NC_{prob} matches with that of the experimental results, we analyze the effect of NC_{prob} on AROW performance in terms of the state transitions. For this reason, Figure 7 displays the

| n_{veh} | NC_{prob} | Percentage of CVs | | |
|-----------|-------------|---------------------|------|------|
| | | 1 | 2 | 3 |
| 4 | 0.1 | 88 | 10.7 | 1.3 |
| | 0.25 | 90.6 | 8.8 | 0.6 |
| 8 | 0.1 | 25.1 | 57.7 | 17.2 |
| | 0.25 | 34.4 | 54.8 | 10.8 |
| 16 | 0.1 | 0.9 | 29.3 | 69.8 |
| | 0.25 | 3.3 | 29.7 | 67 |

TABLE VI: Percentages of competing CAVs (CVs) during AROW rounds for non-compliance scenarios ($NC_{prob} = 0.1$, $NC_{prob} = 0.25$)

state transition matrices in the form of heat maps for different values of n_{veh} and NC_{prob} . Most transitions and trends in the heat maps in Figures 5 and 7 are similar except for the transitions involving NC_{stages} . The first major difference is that the heat maps in Figure 7 contain non-zero transitions in $N_8 : (S_{22}, v) \xrightarrow{a_8} (S_0, v')$, $N_7 : (S_{22}, v) \xrightarrow{a_7} (S_1, v')$, $N_{11} : (S_{23}, v) \xrightarrow{a_{11}} (S_0, v')$, $N_{10} : (S_{23}, v) \xrightarrow{a_{10}} (S_1, v')$, $N_{13} : (S_{31}, v) \xrightarrow{a_{13}} (S_1, v')$, $N_{14} : (S_{31}, v) \xrightarrow{a_{14}} (S_0, v')$, $N_{16} : (S_{32}, v) \xrightarrow{a_{16}} (S_1, v')$, and $N_{17} : (S_{32}, v) \xrightarrow{a_{17}} (S_0, v')$, due to NC_{prob} , as opposed to the same transitions which were all 0% in the heat maps in Figure 5 due to full compliance.

It has been mentioned that in the case of non-zero NC_{prob} , AROW within every compliant competing CAV utilizes $AROW_{thresh}$ so that in the cases of non-compliance by some other CAV(s), it does not need to withdraw from using AROW altogether and transition to S_0 but instead re-attempt AROW until (4) is being satisfied. This is the reason why the transitions $N_5 : (S_{21}, v) \xrightarrow{a_5} (S_{22}, v')$ and $N_6 : (S_{21}, v) \xrightarrow{a_6} (S_{23}, v')$ yield higher percentages with $NC_{prob} = 0.25$ than $NC_{prob} = 0.1$, which in turn yields higher percentages than $NC_{prob} = 0$. The same reasoning is also responsible for the increase in percentages of $N_9 : (S_{22}, v) \xrightarrow{a_9} (S_{31}, v')$, and $N_{12} : (S_{23}, v) \xrightarrow{a_{12}} (S_{32}, v')$ in the cases of $NC_{prob} = 0.25$ than $NC_{prob} = 0.1$.

Next, for any n_{veh} in Figure 7, as NC_{prob} increases, so does the percentage of non-compliance related transitions from any of the NC_{stages} . For example, it can be observed that N_7 is higher for $NC_{prob} = 0.25$ as compare to that for $NC_{prob} = 0.1$. The same is the case with N_8 , N_{10} , N_{11} , N_{13} , N_{14} , N_{16} , and N_{17} . This can also be understood by analyzing that for any n_{veh} , the total non-compliance percentage by taking the sum of N_7 , N_8 , N_{10} , N_{11} , N_{13} , N_{14} , N_{16} , and N_{17} increases with the rise in NC_{prob} according to the $P(\exists NC')$ analysis earlier. Also, as n_{veh} rises, this denotes that there will be more competing CAVs to HV and thus the percentages of the above-mentioned transitions increase even further.

In addition, it can also be observed that for $n_{veh} = 8, 16$, the heat maps display a higher percentages for N_{13} and N_{16} as compared to N_{14} and N_{17} , respectively. As n_{veh} increases, so does the percentage of $N_3 : (S_1, v) \xrightarrow{a_3} (SW, v')$ since there is a higher probability that HV would encounter CAVs competing for AROW when it arrives at the SC-I. This in turn explains the increase in the percentages of $N_{21} : (SW, v) \xrightarrow{a_{21}} (S_{31}, v')$ and $N_{23} : (SW, v) \xrightarrow{a_{23}} (S_{32}, v')$ where HV goes from SW directly to S_{31} or S_{32} towards the end of the successful preceding AROW. Recalling the logic behind $AROW_{thresh}$, this means that as the HV arrives at S_{31} or S_{32} , its $AROW_{thresh}$

is still 0, and thus if there is non-compliance and (4) holds true, HV would restart its AROW and use N_{13} and N_{16} to transition to S_1 rather than transitioning to S_0 and disable its AROW. This behavior can be observed for both non-zero NC_{prob} values. For the same reason, the percentages of N_8 and N_{11} are higher than that of N_7 and N_{10} because as HV reaches S_{22} or S_{23} , it is probable that due to the non-compliance in the previous AROW round, the $AROW_{count}$ is close to reaching $AROW_{thresh}$, and thus a non-compliance here would mean that HV would disable its AROW. These behaviors are not viewable in the case of $n_{veh} = 4$ simply because there are not enough CAVs in the scenario to force HV to transition to SW upon arriving at the SC-I.

Finally, Figure 7 also shows that for any n_{veh} , the percentage of $N_{15} : (S_{31}, v) \xrightarrow{a_{15}} (S_{41}, v')$ and $N_{18} : (S_{32}, v) \xrightarrow{a_{18}} (S_{42}, v')$ reduces with the increase of NC_{prob} and that is a direct consequence of NC_{prob} as it reduces the probability of a successful AROW completion.

3) *AROW Impact based on Evaluation Metrics*: The impact of AROW is evaluated on the basis of ambiguity reduction and fairness. The main contribution of AROW is to reduce the ambiguity that drivers may face upon arriving at the SC-I at close time intervals to each other. This in turn can allow fairness in terms of SC-I crossing priority assignments. In this regard, the two metrics are mentioned below:

- For ambiguity reduction, we calculate the frequency of ambiguous instances (n_{amb}) at SC-I where vehicles arrive at close intervals of each other. n_{amb} is characterized by the number of false starts by vehicles in situations where the right-of-way is not clearly evident.
- For fairness-based metric, the vehicle clearance time ($T_{clearance}$) is calculated for a set of leading competing vehicles S_{CV} at an intersection that arrive within T_1 of each other. This is the time difference between the first vehicle in S_{CV} entering the junction and the last vehicle in S_{CV} exiting the junction. SC-I junction can be described as the region within the SC-I past the stop sign. $T_{clearance}$ can be described as:

$$T_{clearance} = \max(S_B) - \min(S_A) \quad (17)$$

where S_A and S_B are the sets for the junction arrival and departure timestamp, respectively.

To avoid any confusion, it should be noted that only those vehicles utilizing AROW are denoted as CAVs. For n_{amb} , AROW is compared to the allway stop intersection management method from SUMO. This method is similar to the real-life human behavior at an SC-I. The default rules of allway stop within SUMO are according to the general right-of-way rules [35]. For AROW, $n_{amb} = 0$ for all cases since CAVs are always aware of their SC-I passing turn. However, same is not the case for allway as there are multiple cases where vehicles have a false start due to ambiguity. Table VII shows the instances of non-zero n_{amb} in allway method for different values of n_{veh} . The column labeled '1' refers to all the cases where for any group of competing vehicles, only one vehicle enters the junction at a time, and thus, $n_{amb} = 0$. As suggested by the percentages under this column, majority

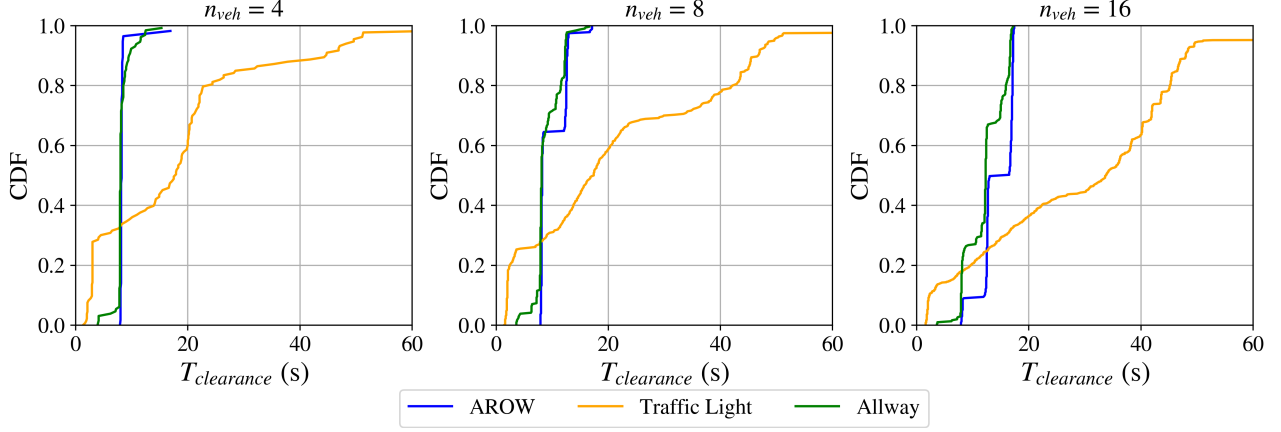


Fig. 8: CDF comparison of vehicle clearance time ($T_{clearance}$) between AROW, traffic light, and allway

| n_{veh} | Competing Vehicles in Allway SC-I | | | Total |
|-----------|-----------------------------------|-------------|----------|-------|
| | (n_{amb}) | | | |
| | 1 | 2 | 3 | |
| 4 | 427 (96%) | 17 (3.8%) | 1 (0.2%) | 445 |
| 8 | 606 (84.5%) | 106 (14.8%) | 5 (0.7%) | 717 |
| 16 | 696 (82.2%) | 143 (16.9%) | 8 (0.9%) | 847 |

TABLE VII: Tabular representation of allway SC-I scenarios with false-starts due to ambiguity (n_{amb})

of the cases within allway occur without ambiguity. However, there are cases where ‘2’ or ‘3’ vehicles out of the competing vehicles enter the SC-I junction due to ambiguity, thus non-zero n_{amb} as shown in their respective columns in the table. Additionally, the percentages of n_{amb} for these columns can be observed to rise with the increase in n_{veh} .

In addition to ambiguity reduction, AROW also promotes fairness among competing vehicles at an SC-I without necessarily causing additional delays. Figure 8 compares the $T_{clearance}$ CDF of AROW to allway and traffic signal methods from SUMO, respectively. The results from traffic light based intersection have been included to serve as a baseline. It is clearly observable from Figure 8 that AROW does not only outperform traffic lights in terms of $T_{clearance}$ but it also yields very similar results to allway for all values of n_{veh} . To analyze the differences numerically, consider the equation below:

$$\Delta A = \int_a^b T_{clearance_1}(t)dt - \int_c^d T_{clearance_2}(t)dt \quad (18)$$

where ΔA is the difference between the areas under the two CDF curves of $T_{clearance}$. Using (18), ΔA between traffic light and AROW is 60.7, 113.7, and 103.5, for $n_{veh} = 4, 8$, and 16, respectively. On the other hand, ΔA between allway and AROW for the same values of n_{veh} is -1.48, 0.2, 1.93, respectively. Thus, this calculation reiterates that AROW performs far better than traffic light in terms of $T_{clearance}$ and it is very similar to that of allway.

VI. CONCLUSION

This study proposes the AROW algorithm to reduce priority-related ambiguity at SC-Is. The algorithm utilizes a cooperative DMS where vehicles use V2X to communicate

with each other. AROW is deployed to run several simulation scenarios involving various levels of CAVs and NC_{prob} values of non-compliance to prove the completeness and robustness of AROW. The paper iterates the accuracy of the proposed algorithm by showing close similarities between the theoretical metrics and experimental results. Finally, AROW is evaluated on the basis of ambiguity mitigation and intersection clearance time as compared to traffic light and allway-stop based intersections from SUMO traffic simulator. AROW is observed to outperform traffic lights and allway in both metrics. As future work, the authors plan to test AROW under real-life conditions by embedding the DMS and the underlying AROW on to the test hardware. Secondly, AROW can be stress-tested under varying levels of congested channels and communication losses to further improve the robustness of the algorithm. Current study assumes that all CAVs are connected, which can be relaxed to show the robustness of AROW in corner cases in the presence of connected and non-connected vehicles. Finally, the timeouts $T1$, $T2$, and $T3$ can be optimized by conducting analysis on communication latencies using different V2X technologies. These optimized timeouts can further accelerate AROW.

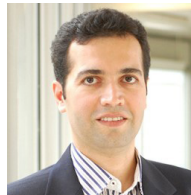
REFERENCES

- [1] C. B. Rafter, B. Anvari, and S. Box, “Traffic responsive intersection control algorithm using gps data,” in *2017 IEEE 20th International Conference on Intelligent Transportation Systems (ITSC)*. IEEE, 2017, pp. 1–6.
- [2] Y. Rahmati and A. Talebpour, “Towards a collaborative connected, automated driving environment: A game theory based decision framework for unprotected left turn maneuvers,” in *2017 IEEE Intelligent Vehicles Symposium (IV)*. IEEE, 2017, pp. 1316–1321.
- [3] L. Blincoe, T. R. Miller, E. Zaloshnja, and B. A. Lawrence, “The economic and societal impact of motor vehicle crashes, 2010 (revised),” Tech. Rep., 2015.
- [4] R. A. Retting, H. B. Weinstein, and M. G. Solomon, “Analysis of motor-vehicle crashes at stop signs in four us cities,” *Journal of Safety Research*, vol. 34, no. 5, pp. 485–489, 2003.
- [5] M.-k. Shi, H. Jiang, and S.-h. Li, “An intelligent traffic-flow-based real-time vehicles scheduling algorithm at intersection,” in *2016 14th International Conference on Control, Automation, Robotics and Vision (ICARCV)*. IEEE, 2016, pp. 1–5.
- [6] E.-H. Choi, “Crash factors in intersection-related crashes: An on-scene perspective,” 2010.

- [7] R. Azimi, G. Bhatia, R. R. Rajkumar, and P. Mudalige, "Stip: Spatio-temporal intersection protocols for autonomous vehicles," in *2014 ACM/IEEE international conference on cyber-physical systems (ICCPs)*. IEEE, 2014, pp. 1–12.
- [8] S. Singh, "Critical reasons for crashes investigated in the national motor vehicle crash causation survey," Tech. Rep., 2015.
- [9] L. Chen and C. Englund, "Cooperative intersection management: A survey," *IEEE transactions on intelligent transportation systems*, vol. 17, no. 2, pp. 570–586, 2015.
- [10] E. Namazi, J. Li, and C. Lu, "Intelligent intersection management systems considering autonomous vehicles: A systematic literature review," *IEEE Access*, vol. 7, pp. 91 946–91 965, 2019.
- [11] Z. Zhong, M. Nejad, and E. E. Lee, "Autonomous and semiautonomous intersection management: A survey," *IEEE Intelligent Transportation Systems Magazine*, vol. 13, no. 2, pp. 53–70, 2020.
- [12] J. B. Kenney, "Dedicated short-range communications (dsrc) standards in the united states," *Proceedings of the IEEE*, vol. 99, no. 7, pp. 1162–1182, July 2011.
- [13] 3GPP, "Evolved universal terrestrial radio access (e-utra); physical layer procedures (v14.7.0)," vol. 3GPP. TS 36.213, June 2018.
- [14] G. Shah, R. Valiente, N. Gupta, S. O. Gani, B. Toghi, Y. P. Fallah, and S. D. Gupta, "Real-time hardware-in-the-loop emulation framework for dsrc-based connected vehicle applications," in *2019 IEEE 2nd Connected and Automated Vehicles Symposium (CAVS)*. IEEE, 2019, pp. 1–6.
- [15] G. Shah, M. Saifuddin, Y. P. Fallah, and S. D. Gupta, "Rve-cv2x: A scalable emulation framework for real-time evaluation of cv2x-based connected vehicle applications," in *2020 IEEE Vehicular Networking Conference (VNC)*. IEEE, 2020, pp. 1–8.
- [16] H.-J. Chang and G.-T. Park, "A study on traffic signal control at signalized intersections in vehicular ad hoc networks," *Ad Hoc Networks*, vol. 11, no. 7, pp. 2115–2124, 2013.
- [17] J.-D. Schmöcker, S. Ahuja, and M. G. Bell, "Multi-objective signal control of urban junctions—framework and a london case study," *Transportation Research Part C: Emerging Technologies*, vol. 16, no. 4, pp. 454–470, 2008.
- [18] D. DeVoe and R. W. Wall, "A distributed smart signal architecture for traffic signal controls," in *2008 IEEE International Symposium on Industrial Electronics*. IEEE, 2008, pp. 2060–2065.
- [19] K. Dresner and P. Stone, "Multiagent traffic management: A reservation-based intersection control mechanism," in *Autonomous Agents and Multiagent Systems, International Joint Conference on*, vol. 3. Citeseer, 2004, pp. 530–537.
- [20] L. Li and F.-Y. Wang, "Cooperative driving at blind crossings using intervehicle communication," *IEEE Transactions on Vehicular technology*, vol. 55, no. 6, pp. 1712–1724, 2006.
- [21] H. Kowshik, D. Caveney, and P. Kumar, "Provable systemwide safety in intelligent intersections," *IEEE transactions on vehicular technology*, vol. 60, no. 3, pp. 804–818, 2011.
- [22] F. Perronnet, A. Abbas-Turki, J. Buisson, A. El Moudni, R. Zeo, and M. Ahmane, "Cooperative intersection management: Real implementation and feasibility study of a sequence based protocol for urban applications," in *2012 15th international IEEE conference on intelligent transportation systems*. IEEE, 2012, pp. 42–47.
- [23] J. Wu, A. Abbas-Turki, and A. El Moudni, "Cooperative driving: an ant colony system for autonomous intersection management," *Applied Intelligence*, vol. 37, pp. 207–222, 2012.
- [24] M. VanMiddlesworth, K. Dresner, and P. Stone, "Replacing the stop sign: Unmanaged intersection control for autonomous vehicles," in *Proceedings of the 7th international joint conference on Autonomous agents and multiagent systems-Volume 3*, 2008, pp. 1413–1416.
- [25] A. A. Hassan and H. A. Rakha, "A fully-distributed heuristic algorithm for control of autonomous vehicle movements at isolated intersections," *International Journal of Transportation Science and Technology*, vol. 3, no. 4, pp. 297–309, 2014.
- [26] G. Shah, S. Shahram, Y. Fallah, D. Tian, and E. Moradi-Pari, "Enabling a cooperative driver messenger system for lane change assistance application," in *2022 IEEE 25th International Conference on Intelligent Transportation Systems (ITSC)*. IEEE, 2022, pp. 4320–4327.
- [27] S. Rajab, S. Bai, S. Saigusa, J. Keller, A. Pradhan, S. Bao, and J. Sullivan, "Driver to driver (d2d) personalized messaging based on connected vehicles: Concept evaluation via simulation," 2017.
- [28] R. Alur and D. L. Dill, "A theory of timed automata," *Theoretical computer science*, vol. 126, no. 2, pp. 183–235, 1994.
- [29] R. Alur, "Timed automata," in *International Conference on Computer Aided Verification*. Springer, 1999, pp. 8–22.
- [30] S. Krauß, P. Wagner, and C. Gawron, "Metastable states in a microscopic model of traffic flow," *Physical Review E*, vol. 55, no. 5, p. 5597, 1997.
- [31] P. A. Lopez, M. Behrisch, L. Bieker-Walz, J. Erdmann, Y.-P. Flötteröd, R. Hilbrich, L. Lücken, J. Rummel, P. Wagner, and E. Wießner, "Microscopic traffic simulation using sumo," in *The 21st IEEE International Conference on Intelligent Transportation Systems*. IEEE, 2018. [Online]. Available: <https://elib.dlr.de/124092/>
- [32] A. Wegener, M. Piórkowski, M. Raya, H. Hellbrück, S. Fischer, and J.-P. Hubaux, "Traci: an interface for coupling road traffic and network simulators," in *Proceedings of the 11th communications and networking simulation symposium*, 2008, pp. 155–163.
- [33] S. International, "Lte vehicle-to-everything (lte-v2x) deployment profiles and radio parameters for single radio channel multi-service coexistence," Society of Automotive Engineers, Standard J3161, 04 2022.
- [34] B. Toghi, M. Saifuddin, H. N. Mahjoub, M. O. Mughal, Y. P. Fallah, J. Rao, and S. Das, "Multiple access in cellular v2x: Performance analysis in highly congested vehicular networks," in *2018 IEEE Vehicular Networking Conference (VNC)*. IEEE, 2018, pp. 1–8.
- [35] U.S. Department of Transportation, Federal Highway Administration, "Manual on uniform traffic control devices (mutcd)," Online, 2003, accessed on March 26, 2023. [Online]. Available: <https://mutcd.fhwa.dot.gov/htm/2003r1/part2/part2b1.htm#section2B04>



Ghayoor Shah is a Ph.D. candidate at the University of Central Florida. He received the B.Sc. degree in Computer Engineering from University of Illinois at Urbana-Champaign in 2018. He has previously worked as a mobility engineering intern at Phantom Auto and as a research intern at Ford Motor Company. His research interests include Connected and Autonomous Vehicles (CAVs), scalability analysis of V2X, and applications of artificial intelligence to cooperative driving.



Yaser P. Fallah is an Associate Professor in the ECE Department at the University of Central Florida. He received the Ph.D. degree from the University of British Columbia, Vancouver, BC, Canada, in 2007. From 2008 to 2011, he was a Research Scientist with the Institute of Transportation Studies, University of California Berkeley, Berkeley, CA, USA. His research, sponsored by industry, USDOT, and NSF, is focused on intelligent transportation systems and automated and networked vehicle safety systems.



Danyang Tian earned her Ph.D. degree in electrical engineering from the University of California, Riverside, in 2018. She is currently a scientist at Honda Research Institute USA, Inc. Her research interests include connected and automated vehicles, vehicular communication systems, and driver behavior modeling, application design and development of connected and automated vehicles, vehicle-to-everything (V2X) communication technologies. She serves as chair in the SAE International V2X Vehicular Applications Technical Committee.



Ehsan Moradi-Pari is a lead principal scientist and communication/data research group lead at Honda Research Institute (HRI-US). His current research is focused on vehicle-to-vehicle (V2V) and vehicle-to-infrastructure (V2I) communications based on short-range communication and cellular technologies. He serves as Honda lead and representative for V2V and V2I precompetitive research such as Vehicle-to-Vehicle Systems Engineering and Vehicle Integration Research for Deployment, Cooperative Adaptive Cruise Control, and 5G Automotive Association (5GAA). He has spearheaded Honda's efforts and preparations to accelerate connected automated vehicle deployment in the United States and the state of Ohio where he led the team to design and deploy the first-of-its-kind smart intersection concept in Marysville, Ohio. Dr. Moradi-Pari has several publications in internationally refereed journals, conference proceedings, and book chapters in the area of designing communication protocols and applications for connected and automated vehicles and modeling/analysis of intelligent transportation systems.